Kinematic viscosity estimates in reversed-field pinch fusion plasmas

Journal of Physics: Conference Series **2397** (2022) 012010 doi:10.1088/1742-6596/2397/1/012010

Kinematic viscosity estimates in reversed-field pinch fusion plasmas

N Vivenzi[1,2], G Spizzo[1,3], M Veranda[1], D Bonfiglio[1,3], S Cappello[1,3] and RFX-mod Team

[1] Consorzio RFX (CNR, ENEA, INFN, Università degli Studi di Padova, Acciaierie Venete SpA), C.so Stati Uniti 4, 35127 Padova, Italy
[2] CRF – University of Padova, Italy
[3] CNR - ISTP Padova, Italy

E-mail: nicholas.vivenzi@studenti.unipd.it

Abstract.
This paper concerns the kinematic viscosity in reversed-field pinch fusion plasmas, including both the study of numerical magneto-hydrodynamics (MHD) simulations and the analysis of RFX-mod experimental data.
In the first part, we study the role of non-uniform time-constant radial viscosity profiles in 3D non-linear visco-resistive MHD simulations. The new profiles induce a moderate damp (for the velocity field) and a correspondent enhancement (for the magnetic field) of the spectral components resonating in the regions where the viscosity is higher.
In the second part, we evaluate the kinematic viscosity coefficient on a wide database of RFX-mod shots according to the transport theories of Braginskii (considering parallel, perpendicular and gyro viscosity coefficients), considering the action on viscosity of ITG modes (ion temperature gradient) and according to the transport theory of Finn. We then exploit the comparison with the visco-resistive MHD simulations (where the visco-resistive dissipation rules the MHD activity) to show that the classical Braginskii perpendicular viscosity produces the best agreement between simulations and data, followed by the Braginskii gyro-viscosity.

Keywords: viscosity, reversed-field pinch, magnetohydrodynamics, fusion plasmas.

Submitted to: *J. Phys.: Conf. Ser.*

Viscosity estimates in RFP fusion plasmas

1. Introduction

In the magneto-hydrodynamics (MHD) modelling of fully ionized plasmas, a "neutral fluid like" viscosity term is introduced in the momentum balance equation to represent momentum transport in the plasma. Viscosity determines, together with resistivity, the dimensionless Hartmann number [1], which quantifies the plasma 'slipperiness' and rules some important aspects of plasma dynamics [2].
This is more evident in the reversed-field pinch (RFP), a toroidal configuration used for magnetic confinement in nuclear fusion research [3]. In this configuration, MHD theory and numerical simulations [4] have played a key role during the last decades, describing the occurrence of helical self-organized states [5, 6], which represent a fundamental feature of RFP plasmas [7, 8]. More recently, the predictions of the model have reached a good level of agreement with the RFX-mod data, being able to predict both the helical twist [9] and the intensity of the perturbed mode [10] of helical states, exploiting the introduction of non-ideal magnetic field boundary conditions. Despite the interest in the RFP plasma viscosity, no unique consensus on either the form of the viscous term or the viscosity coefficient evaluation in RFP plasmas still exists [1]. In fact, the experimental estimates [11, 12, 13, 14, 15] carried on according to classical [16] or turbulent transport [17, 18] theory display orders of magnitude differences. In addition, a more recent study [19] has shown the electrostatic turbulence to play a central role in fusion plasmas momentum transport. These considerations motivate further studies to assess a viscosity estimate in RFP plasmas.
This paper has two main goals: to study the effects of non-uniform viscosity profiles in visco-resistive MHD simulations and to figure out which among the momentum transport theories (and the related viscosity estimates) produces the best agreement between MHD simulations and experimental data. In Sec. 2 the visco-resistive MHD model and the SpeCyl code are introduced, in Sec. 3 we perform a sensitivity study in SpeCyl simulations to test the effect of non-uniform radial viscosity profiles. In Sec. 4 the kinematic viscosity is evaluated according to the main transport theories, while in Sec. 5 we assess which among the transport theories produces the highest agreement level between simulations and experimental data. Discussion and conclusions follow in Sec. 6.

2. Visco-resistive magnetohydrodynamics model

In this paper, reversed-field pinch fusion plasmas are studied using the 3D nonlinear visco-resistive magneto-hydrodynamics (MHD) model. The model is obtained considering single fluid MHD equations, assuming a constant mass density and neglecting the effects introduced by the pressure gradient in the equation of motion. Since we consider low β plasmas and we focus on current driven instabilities, the latter hypothesis is satisfied. The model consists of the following equations, written in dimensionless units:

$$\frac{\partial \mathbf{v}}{\partial t} + (\mathbf{v}\cdot\nabla)\,\mathbf{v} = \mathbf{j}\times\mathbf{B} + \nu\nabla^2\mathbf{v}, \tag{1}$$

$$\frac{\partial \mathbf{B}}{\partial t} = \nabla\times(\mathbf{v}\times\mathbf{B}) - \nabla\times(\eta\mathbf{j})\,, \tag{2}$$

$$\nabla\cdot\mathbf{B} = 0, \tag{3}$$

$$\mathbf{j} = \nabla\times\mathbf{B}, \tag{4}$$

where space, time and magnetic field are normalized respectively to plasma minor radius a, Alfvén time τ_A and on-axis magnetic field B_0. In these units, resistivity and viscosity (that represent the transport coefficients of the model) are expressed naturally as the inverse of the Lundquist number $\eta = \tau_r/\tau_A = S^{-1}$ and of the viscous Lundquist number $\nu = \tau_\mu/\tau_A = M^{-1}$.
SpeCyl [4] is a numerical code which performs the solution of the visco-resistive model (1 - 4) in cylindrical geometry, exploiting a spectral formulation in the axial and azimuthal coordinates and a finite differences method in the radial one. This code has successfully undergone to a cross-benchmark nonlinear verification study [20] with the 3D finite volume MHD code PIXIE3D [21]. So far in the SpeCyl code, the transport coefficients (η, ν) have been considered to be constant in time and a simple radial profile is commonly assumed for both resistivity $\eta(r) = \eta_0\,(1 + 20r^{10})$ and viscosity $\nu(r) = \nu_0$.
With a proper change of coordinates $(t, \mathbf{v}) \rightarrow \left(\bar{t} = \sqrt{\eta/\nu}\,t, \bar{\mathbf{v}} = \sqrt{\nu/\eta}\,\mathbf{v}\right)$ and the introduction of the Prandtl $P = \nu/\eta$ and the Hartmann numbers $H = 1/\sqrt{\eta\nu}$, the plasma dynamics (1 - 4) is shown to depend only on the latter dimensionless coefficient, if the inertia term in (1) becomes negligible, [2]. Therefore, the Hartmann number turns out to be the ruling parameter of the MHD activity [22], highlighting the joint role of both resistivity and viscosity in determining the plasma dynamics and the need for an experimental evaluation of both the transport coefficients. This is a challenging task, especially for the viscosity coefficient, and it represents one of the main problems in the laboratory plasma application of MHD theory [1].

3. Effect of non-uniform viscosity radial profiles in MHD simulations

In a recent work on visco-resistive MHD simulations [23], the systematic variation of resistivity and viscosity profiles near the reversal is found to influence the excitation of $m = 0$ modes during the RFP sawtooth crash. In this section, we investigate the effects of non-uniform time-constant, radial viscosity profiles in 3D non-linear MHD simulations, focusing the analysis on the time-average of velocity and magnetic field spectral components. The case of viscosity profile resembling the functional dependence indicated by Braginskii for the perpendicular viscosity $\nu_\perp^{Brag}$ is here presented, since the RFP dynamics is determined by magnetic instabilities and fluid convection, both perpendicular to the magnetic field. For the sake of completeness, other profiles were also considered (see Sec. 4). In this study, we compare SpeCyl simulations with either flat $(\nu(r) = \nu_0)$ (the most frequent setting in recent simulations studies [9, 10]) or

Viscosity estimates in RFP fusion plasmas

Braginskii-like ($\nu/\nu_0 = 1 + 20r^3\cos(1.6r)$) viscosity profiles respectively: the latter is larger by an average factor 2.8, and up to 4 in the edge region, Fig. 1 (a).
In the two simulations we set: $\eta_0 = 10^{-6}$, $\nu_0 = 10^{-4}$, ideal magnetic field boundary conditions $b_r(a) = 0$ and the same resistivity profile: $\eta(r) = \eta_0\,(1 + 20r^{10})$. The different viscosity profile setting does not significantly modify the axis-symmetric components of the magnetic field, Fig. 1 (b), (c).

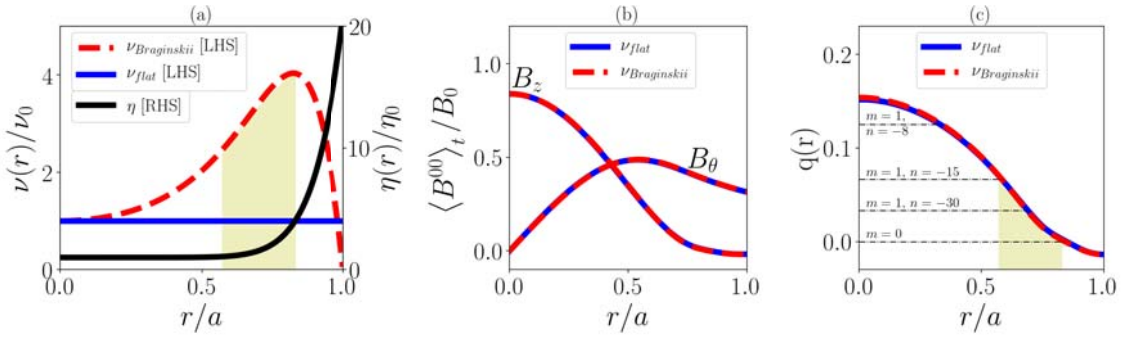

Figure 1. SpeCyl simulations settings for resistivity and viscosity (a), time average axisymmetric fields (b), safety factor (c) comparison for the flat and perpendicular Braginskii viscosity profile. The resonance of $m = 0$ and $m = 1$ secondary modes corresponds to the highlighted region where the Braginskii viscosity profile is larger than the flat one.

Comparing the time dependence of the kinetic $W_k(t)$ and the magnetic energy $W_M(t)$ of the $m = 1$ dominant and secondary modes (being m and n the poloidal and axial wave numbers) shows that the basic RFP sawtoothing dynamics, i.e. quasi-periodic emergence of a dominant mode in the MHD spectrum, is unchanged by the viscosity profiles, Fig. 2 (a) - (d). However, the time-average energy spectrum ratio (Fig. 3) highlights a moderate damp of the $m = 1$ and $m = 0$ velocity spectral components with respect to the simulations with a radially constant viscosity profile. In particular, the damp is greater for those components resonating in the spatial regions where the viscosity profile is higher. Furthermore, an increased MHD activity magnetic activity of the $m = 1$ spectral components is confirmed by the v_z and b_z eigen-functions radial profile, Fig. 2 (e) - (h). This is consistent with a simple picture of velocity and magnetic field interplay: the plasma flow counteracts the growth of magnetic perturbations and vice-versa [24].
The case of the $m = 0$ modes magnetic energy is less clear (Fig. 3 (b)): although the majority of the $m = 0$ modes displays an increase of the magnetic energy, it is not possible to identify a precise trend. In this case, the flow 'reducing action' on the magnetic instabilities is less effective because at the reversal (the resonance region of $m = 0$ modes) the flow itself is small, being evaluated near the edge, where the no-slip boundary condition is assumed in this simulation ($v_z^{00}(a) = 0$). In addition, the modes non-linear interaction may possibly contribute to the $m = 0$ modes reduced enhancement.

Viscosity estimates in RFP fusion plasmas

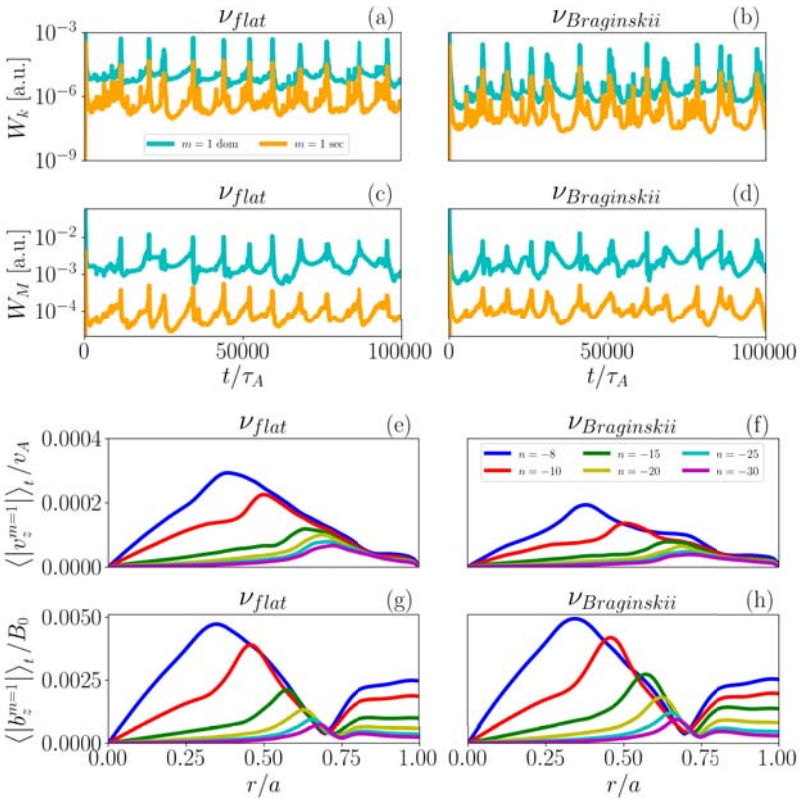

Figure 2. Viscosity profiles (ν_{flat} and $\nu_{Braginskii}$) effect comparison in SpeCyl simulations. The introduction of the Braginskii viscosity profile produces: a damp of $m = 1$ dominant and secondary modes kinetic energy W_k (a, b) and of $m = 1$ axial velocity eigen-functions $v_z^{m=1}$ (e, f) and a slight enhancement of magnetic energy W_M (c, d) and axial component magnetic field $v_z^{m=1}$ (g, h), more evident for $n \leq -15$ modes.

Viscosity estimates in RFP fusion plasmas

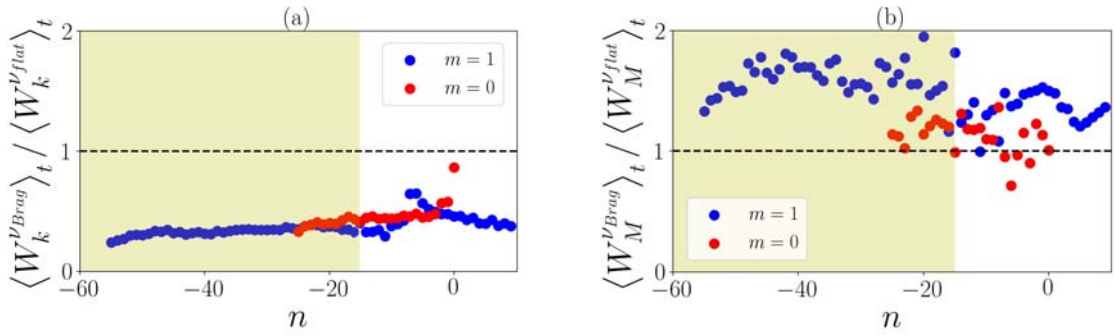

Figure 3. The time-average energy ratio between the Braginskii and uniform viscosity profile for each $m = 0$ (•) and $m = 1$ (•) spectral component shows: a damp of the kinetic energy, for both the $m = 1$ and the $m = 0$ modes (a) and a more noticeable enhancement of the magnetic energy for the $m = 1$, $n \leq -15$ secondary modes (blue markers highlighted in in the figure) (b). No definite trend is shown for the $m = 0$ modes, although the majority of them shows a magnetic energy enhancement.

4. RFX-mod plasmas viscosity estimates

In this section, we estimate the kinematic viscosity coefficient according to the various momentum transport theories developed for hot magnetized plasmas (briefly sketched out in the next paragraphs): classical Braginskii (parallel $\nu_{\parallel}$ (5), perpendicular $\nu_{\perp}$ (6), gyro-viscous $\nu_{\times}$ (7)), ITG ν_{ITG} (8) and Finn ν_{Finn} (9) viscosity.

The *classical viscosity* is derived from the closure procedure [25], [26] of the Braginskii equations, needed to solve the problem of MHD equations incompleteness [27]. In a plasma, this procedure considers binary Coulomb collisions as the microscopic mechanism that originates momentum transport. Despite its tensorial nature, the latter is usually represented by means of three Braginskii viscosity coefficients [16]: $\nu_{\parallel}$ and $\nu_{\perp}$ which rule, respectively the variation along/perpendicular to the magnetic field lines of velocity components parallel/perpendicular to the magnetic field and $\nu_{\times}$ [28] which originates from a magnetic field - temperature gradient interplay, not providing a viscous heating effect.

The *ion temperature gradient (ITG) viscosity* [18] is caused by an ion temperature gradient driven mode that damps the velocity fluctuations (associated to the tearing modes) originating an anomalous ion heating (i. e. anomalous viscosity effect).

The *Finn anomalous viscosity* [17] models the momentum transport in a stochastic magnetic field by sound waves propagation, considering a stochastic magnetic diffusion coefficient according to the Rechester-Rosenbluth model [29].

In literature, measurements of the viscosity coefficient in RFP plasmas are available, based on the plasma response to a biased probe and on the modes braking due to resonant magnetic perturbation (RMP), [14]. However, in this work, we focused on an indirect estimate of the kinematic viscosity, exploiting formulas in App. A and a wide database of RFX-mod experimental data [30], [31]. RFX-mod is a toroidal device, with major radius $R_0 = 2\,\mathrm{m}$ and minor radius $a = 0.459\,\mathrm{m}$, able to operate

Viscosity estimates in RFP fusion plasmas

in both tokamak and RFP configuration [32]. The database we considered amounts to 243 shots in RFP configuration, including both hydrogen and deuterium plasmas, spanning the ranges: $130\,\mathrm{kA} \leq I_p \leq 2\,\mathrm{MA}$ for the plasma current, $0.15\,\mathrm{T} \leq B_0 \leq 2.0\,\mathrm{T}$ for the on-axis magnetic field, $60\,\mathrm{eV} \leq T_e \leq 1.1\,\mathrm{KeV}$ for the electron temperature and $3.5\times10^{18}\,\mathrm{m}^{-3} \leq n_e \leq 2.2\times10^{20}\,\mathrm{m}^{-3}$ for the electron density). The electron temperature T_e is measured by the Thomson scattering diagnostic [33], the ion temperature is assumed $T_i = 0.5T_e$, the electron density n_e is measured by the interferometer [34] and $Z_{eff} = 1.5$ is assumed, [35]. The magnetic field perturbations involved in the Finn viscosity are evaluated exploiting the NCT code (NewComb Toroidal algorithm), [36].

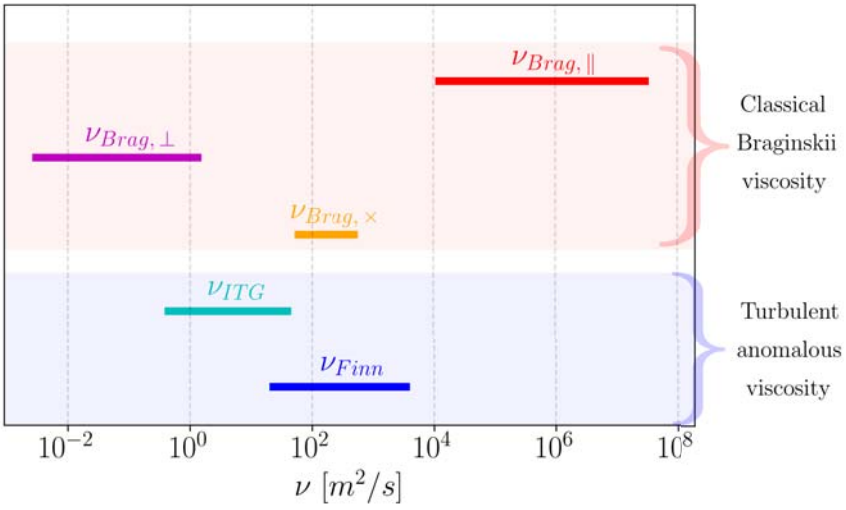

Figure 4. Range of the kinematic viscosity coefficient on RFX-mod plasmas, according to classical (Braginskii) or turbulent (ITG, Finn) theories.

Fig. 4 shows orders of magnitude differences in the range of the different viscosity estimates, discussed in Sec. 5. In particular, we preliminary notice that the parallel Braginskii viscosity $\nu_{\parallel}$ interval values have no overlap with any of the other estimates. On the contrary, the perpendicular viscosity $\nu_{\perp}$ overlaps with the ITG viscosity interval ν_{ITG}, while the gyro-viscosity, the ITG viscosity ν_{ITG} the Finn viscosity ν_{Finn} have comparable orders on the RFX-mod database. This makes it difficult to make a comparison based solely on the viscosity absolute value and stimulates the search for a comparison method that takes into account also the functional dependencies of the viscosity coefficients (see Sec. 5).

5. MHD simulations and experimental data comparison

The aim of this section is to figure out the model for viscosity with the highest adherence to experimental data. To reach this goal, we first estimate the Hartmann number (using the Spitzer resistivity (10) [37] and the five estimates of viscosity from Sec. 4) and we compute the power-law scaling ($y = CX^{\alpha}$) of the normalized temporal scales of

reconnection events $\bar{\tau}_{crash}$ and of $m = 0$, $m = 1$ secondary modes as function of the Hartmann number, which rules the MHD dynamics. For the first scaling, we consider the normalization $\bar{\tau}_{crash} := \sqrt{\eta/\nu}\,\tau_{crash}$: the normalization factor comes from the change of coordinates described in [2] and it is required to evaluate the scaling on the Hartmann number. We estimate the reconnection time τ_{crash} as the interval between the maximum and the minimum value of the edge axial magnetic field, during a reconnection event [38]. For the second and the third scalings, we consider the following quantities to represent the secondary modes:

$$b^z_{0,sec}(a) := \sqrt{\sum_{\substack{-9\leq n\leq -1\\ n\neq -7}} b^z_{0,n}(a)^2}, \qquad b^z_{1,sec}(a) := \sqrt{\sum_{-20\leq n\leq -8} b^z_{1,n}(a)^2},$$

where the $m = 0$, $n = -7$ mode is excluded to avoid considering toroidal effects, in the comparison with the cylindrical code SpeCyl. In Fig. 5, the plots of $\bar{\tau}_{crash}$, $m = 0$ and $m = 1$ secondary modes as function of the five different evaluations of the Hartmann number are shown. The same scalings are computed also for a wide database of SpeCyl simulations (with flat viscosity profile), varying both the absolute values of the dimensionless transport coefficients and the intensity of non-ideal magnetic field boundary conditions [22]. In this case the Hartmann number is determined by the input central values of dimensionless resistivity η_0 and viscosity ν_0: $H_{SpeCyl} := 1/\sqrt{\eta_0\nu_0}$. The fit correlation coefficient r and the scaling slope α values are shown in Tab. 1, referring to both simulations and experimental data.

	α			r		
	$\bar{\tau}_{crash}$	$b^z_{0,sec}(a)/B_0$	$b^z_{1,sec}(a)/B_0$	$\bar{\tau}_{crash}$	$b^z_{0,sec}(a)/B_0$	$b^z_{1,sec}(a)/B_0$
H_{SpeCyl}	0.72 ± 0.05	-0.27 ± 0.05	-0.35 ± 0.03	0.84	-0.76	-0.90
$H_\perp$	0.74 ± 0.02	-0.240 ± 0.009	-0.204 ± 0.004	0.84	-0.69	-0.80
$H_\times$	1.21 ± 0.03	-0.34 ± 0.01	-0.300 ± 0.006	0.84	-0.67	-0.76
$H_\parallel$	1.68 ± 0.09	-	-	0.58	-0.35	-0.35
H_{ITG}	0.95 ± 0.03	-0.24 ± 0.01	-0.218 ± 0.005	0.70	-0.64	-0.70
H_{Finn}	1.14 ± 0.05	-0.33 ± 0.01	-0.271 ± 0.007	0.82	-0.58	-0.61

Table 1. Scaling slope (with uncertainty) and correlation coefficient for the power-law fit of normalized temporal scales of reconnection events and secondary ($m = 0$ and $m = 1$) modes as function of the Hartmann number for both SpeCyl simulations and experimental data evaluation. The highest correlation coefficient and the scaling slope with the best agreement with the simulations are highlighted.

Analyzing the values of the correlation coefficient r we notice that: $H_\parallel$ has little correlation with the secondary modes, while the ITG and Finn estimates of the viscosity produce a correlation coefficient lower than the remaining cases, so these estimates do not represent the best possible choice for the viscosity coefficient evaluation. In support of this, we list some drawbacks related to the Finn viscosity estimate. The correlation values of the scalings

Viscosity estimates in RFP fusion plasmas

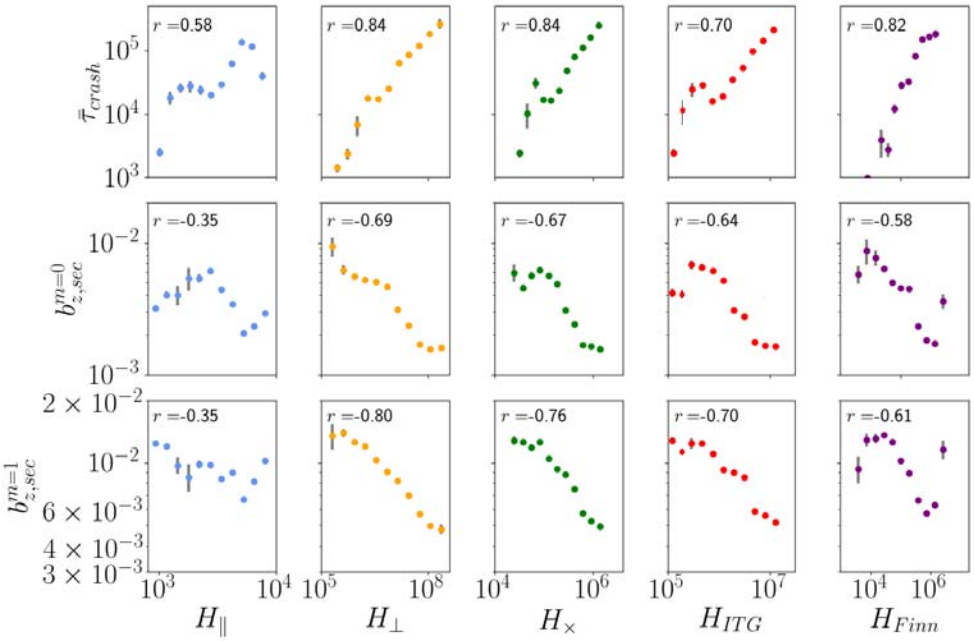

Figure 5. Plot of reconnection events time scale, $m = 0$ and $m = 1$ secondary modes as function of the Hartmann number, evaluating the kinematic viscosity according to the momentum transport theories, described in Sec. 4. For each plot the scaling regression coefficient r is reported. Data are averaged over equal logarithmic intervals of the Hartmann number.

involving $m = 0$ and $m = 1$ secondary modes are lower than in the other cases, despite the definition of the viscosity as function of the secondary modes itself. The hypothesis of quasi-linear response to magnetic field perturbation is rarely satisfied [19], as the hypothesis of uniformly chaotic transport [29], since more recent studies have shown the non-uniformly chaotic and sub-diffusive nature of transport in RFP plasmas [39], [40]. We also notice that the estimate carried on in [14] displays a non-constant anomaly with respect to the classical viscosity $\nu_{\perp}$, which strongly depends on the plasma current.

We observe that the estimate $\nu_{\perp}$ maximizes the correlation of all quantities, followed by $\nu_{\times}$. In addition, $\nu_{\perp}^{Brag}$ and $\nu_{\times}^{Brag}$ display a good level of adherence for the scaling slope (α) of the reconnection events temporal scale $\bar{\tau}_{crash}$ and $m = 1$ secondary modes respectively. The quantitative comparison between simulations and experimental data (Fig. 6) shows that the experimental data match quite well the decreasing trend (at high Hartmann) of the simulations, however displaying a non monotonous trend of $m = 0$ modes for the $\nu_{\times}$ (Fig. 6 (a)) and the existence of an offset in the scaling involving $\nu_{\perp}$ (Fig. 6 (b), (d)). A comparison of the power-law fitting regression coefficients showed that the offset corresponds to a multiplicative factor $\delta \sim 250$ for the perpendicular Braginskii viscosity. Furthermore, we observe that the anomaly factor δ shows a slight variation in the $m = 0$ and $m = 1$ secondary modes scaling, as the Hartmann number is varied.

In the case of the perpendicular viscosity even the domains in the Hartmann number of SpeCyl simulations and experimental data differ significantly. To overcome this difference is a hard task, since the computational time of the simulations increases as the Hartmann number

is increased, while experimental data points with lower $H_\perp$ would require high density, low plasma current and low temperature shots (6), (10), beyond the RFX-mod operational limits.

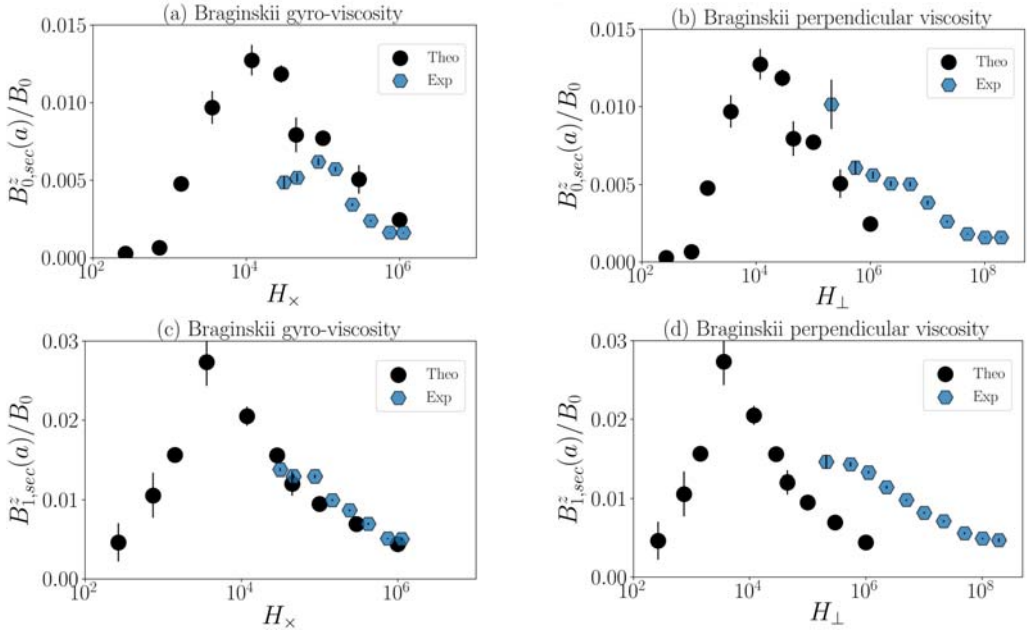

Figure 6. Plot of $m = 0$ and $m = 1$ secondary modes as function of the Hartmann number, evaluated considering perpendicular (b), (d) and gyro (a), (c) Braginskii viscosity, comparing SpeCyl simulations and experimental data. Simulations and data are averaged over equal logarithmic intervals.

6. Summary and final remarks

In this paper, we analyzed the role of the viscosity profile in visco-resistive MHD simulations and we estimated the kinematic viscosity coefficient in RFP fusion plasmas, on the basis of a wide database of RFX-mod shots and according to the main transport theories applied in RFP research. We finally discuss the experimental evaluations exploiting the comparison with SpeCyl visco-resistive MHD simulations.

In the first part, we performed a sensitivity study to assess the effect of a non-uniform viscosity in visco-resistive MHD simulations. In particular, we compared the uniform viscosity and the Braginskii-like viscosity profiles. The latter produces a moderate damp of the flow and an enhancement of magnetic field spectral components resonating in the regions where the viscosity is higher. The enhancement of magnetic fluctuations may increase the level of transport associated to stochastic field lines, and possibly decrease the strength of the $m = 0$ barrier, routinely observed at the edge. No significant differences are observed for the MHD equilibrium, as for the RFP sawtoothing activity.

In the second part, we evaluated the kinematic viscosity relative to a RFX-mod database using a set of different transport theories: classical, ITG and Finn. Exploiting the comparison with SpeCyl simulations, we identify $\nu_\times$ and $\nu_\perp$ as the coefficients which show the best agreement between simulations and data scaling laws. However, a refined quantitative comparison showed the existence of an important offset between the simulation and experimental data scaling for the perpendicular Braginskii viscosity, which would correspond to a multiplicative factor

$\delta \sim 250$, slightly dependent on the Hartmann number.
Many factors can contribute to the origin of the difference in the scaling coefficients, both from the numerical and the experimental side. In SpeCyl simulations, the role of the viscosity profile (as shown in Sec. 3) and the effect of an axisymmetric flow [22] should be mentioned. From the experimental point of view, the possibility of an effective viscosity which is given by the composition of two different coefficients ($\nu_\perp$ and $\nu_\times$) can not be discarded. Also the resistivity can contribute to the difference. Despite in [41] and [42] a remarkable agreement is shown between the Spitzer estimate and the experimental measurements of the resistivity during magnetic reconnection experiments in collisional regime, a recent work [43] has pointed out the need for an order of magnitude anomaly of the resistivity in order to obtain a quantitative agreement between the linear resistive MHD model predictions and resonant modes growth rate measurements on the EXTRAP T2R reversed-field pinch device.
The latter considerations motivate future studies regarding both resistivity and viscosity to understand the origin of the anomaly.

A. Formulas to evaluate plasma viscosity and resistivity

Braginskii viscosity, [16]:

$$\nu_\parallel = 34.6\pi^{3/2}\frac{\epsilon_0^2}{e^4 m_p^{1/2}}\frac{T_i^{5/2}}{Z_{eff}^4 \ln\Lambda \gamma^{1/2} n_i} \propto \frac{T_i^{5/2}}{n_i} \tag{5}$$

$$\nu_\perp = \frac{1}{8\pi^{3/2}}\frac{m_p^{1/2}e^2}{\epsilon_0^2}\frac{\gamma^{1/2} n_e \ln\Lambda}{T_i^{1/2}B^2} \propto \frac{n_e}{T_i^{1/2}B^2} \tag{6}$$

$$\nu_\times = 1.25\frac{1}{e}\frac{T_i}{Z_{eff}B} \propto \frac{T_i}{B} \tag{7}$$

ITG viscosity, [18]:

$$\nu_{ITG} = 1.08\times 10^{-4}\frac{\gamma^{1/2}T_e T_i^{1/2}}{Z_{eff}a_T^{3/4}a_B^{1/4}B^2} \propto \frac{T_e T_i^{1/2}}{B^2}, \quad a_T = 20\,\mathrm{cm}, \quad a_B = 80\,\mathrm{cm} \tag{8}$$

Finn viscosity, [14]:

$$\nu_{Finn} = c_s L_C \sum_{m,n}\left(\frac{b^r_{m,n}}{B}\right)^2 \propto T_e^{1/2}\sum_{m,n}\left(\frac{b^r_{m,n}}{B}\right)^2 \tag{9}$$

evaluating the sound speed $c_s = \sqrt{\frac{\gamma_e Z_{eff}T_e + \gamma_i T_i}{M_i}}$ with $\gamma_e = 1$, $\gamma_i = 3$ and a constant auto-correlation length $L_C = 1.4\,\mathrm{m}$, [44].
Spitzer resistivity, [37]:

$$\eta_\parallel = 0.51\frac{m_e}{n_e e^2 \tau_e} = \frac{0.06}{\pi^{3/2}}\frac{m_e^{1/2}e^2}{\epsilon_0^2}\frac{Z_{eff}\ln\Lambda}{T_e^{3/2}} \propto T_e^{-3/2} \tag{10}$$

In formulas (5 - 10) we evaluate the mass number: $\gamma = 1$ for hydrogen shots, and $\gamma = 2$ for deuterium shots, while the Coulomb logarithm spans the range $13.5 \leq \ln\Lambda \leq 18.7$, in the RFX-mod database shots.

References

[1] D. Montgomery. Magnetohydrodynamic stability thresholds as a function of Hartmann number and pinch ratio. *Plasma Physics and Controlled Fusion*, 34(6):1157–1162, Jun 1992.

[2] S. Cappello and D. F. Escande. Bifurcation in Viscoresistive MHD: The Hartmann Number and the Reversed Field Pinch. *Phys. Rev. Lett.*, 85:3838–3841, Oct 2000.

[3] L. Marrelli, P. Martin, M. E. Puiatti, J. S. Sarff, B. E. Chapman, J. R. Drake, D. F. Escande, and S. Masamune. The reversed field pinch. *Nuclear Fusion*, 61(2):023001, 2021.

[4] S. Cappello and D. Biskamp. Reconnection processes and scaling laws in reversed field pinch magnetohydrodynamics. *Nuclear Fusion*, 36(5):571, 1996.

[5] S. Cappello and R. Paccagnella. Nonlinear plasma evolution and sustainment in the reversed field pinch. *Physics of Fluids B: Plasma Physics*, 4(3):611–618, 1992.

[6] J. M. Finn, R. Nebel, and C. Bathke. Single and multiple helicity ohmic states in reversed-field pinches. *Physics of Fluids B: Plasma Physics*, 4(5):1262–1279, 1992.

[7] R. Lorenzini, E. Martines, P. Piovesan, D. Terranova, P. Zanca, M. Zuin, A. Alfier, D. Bonfiglio, F. Bonomo, A. Canton, S. Cappello, L. Carraro, R. Cavazzana, D. F. Escande, A. Fassina, P. Franz, M. Gobbin, P. Innocente, L. Marrelli, R. Pasqualotto, M. E. Puiatti, M. Spolaore, M. Valisa, N. Vianello, P. Martin, and RFX-mod team and collaborators. Self-organized helical equilibria as a new paradigm for ohmically heated fusion plasmas. *Nature Physics*, 5:570–574, 2009.

[8] P. Piovesan, M. Zuin, A. Alfier, D. Bonfiglio, F. Bonomo, A. Canton, S. Cappello, L. Carraro, R. Cavazzana, D. F. Escande, A. Fassina, M. Gobbin, R. Lorenzini, L. Marrelli, P. Martin, E. Martines, R. Pasqualotto, M. E. Puiatti, M. Spolaore, M. Valisa, N. Vianello, P. Zanca, and the RFX-mod Team. Magnetic order and confinement improvement in high-current regimes of RFX-mod with MHD feedback control. *Nuclear Fusion*, 49(8):085036, Jul 2009.

[9] D. Bonfiglio, M. Veranda, S. Cappello, D. F. Escande, and L. Chacón. Experimental-like Helical Self-Organization in Reversed-Field Pinch Modeling. *Phys. Rev. Lett.*, 111:085002, Aug 2013.

[10] M. Veranda, D. Bonfiglio, S. Cappello, D. F. Escande, F. Auriemma, D. Borgogno, L. Chacón, A. Fassina, P. Franz, M. Gobbin, D. Grasso, and M. E. Puiatti. Magnetohydrodynamics modelling successfully predicts new helical states in reversed-field pinch fusion plasmas. *Nuclear Fusion*, 57(11):116029, Aug 2017.

[11] A. F. Almagri, J. T. Chapman, C. S. Chiang, D. Craig, D. J. Den Hartog, C. C. Hegna, and S. C. Prager. Momentum transport and flow damping in the reversed-field pinch plasma. *Physics of Plasmas*, 5(11):3982–3985, 1998.

[12] B. E. Chapman, R. Fitzpatrick, D. Craig, P. Martin, and G. Spizzo. Observation of tearing mode deceleration and locking due to eddy currents induced in a conducting shell. *Physics of Plasmas*, 11(5):2156–2171, 2004.

[13] L. Frassinetti, S. Menmuir, K. E. J. Olofsson, P. R. Brunsell, and J. R. Drake. Tearing mode velocity braking due to resonant magnetic perturbations. *Nuclear Fusion*, 52(10):103014, Sep 2012.

[14] R. Fridström, B. E. Chapman, A. F. Almagri, L. Frassinetti, P. R. Brunsell, T. Nishizawa, and J. S. Sarff. Dependence of Perpendicular Viscosity on Magnetic Fluctuations in a Stochastic Topology. *Phys. Rev. Lett.*, 120:225002, May 2018.

[15] D. Craig, E. H. Tan, B. Schott, J. K. Anderson, J. Boguski, D. J. Den Hartog, T. Nishizawa, M. D. Nornberg, and Z. A. Xing. Intrinsic flow and tearing mode rotation in the RFP during improved confinement. *Physics of Plasmas*, 26(7):072503, 2019.

[16] S. I. Braginskii. *Transport processes in a plasma*, volume 1. Consultants Bureau, New York, 1965.

[17] J. M. Finn, P. N. Guzdar, and A. A. Chernikov. Particle transport and rotation damping due to stochastic magnetic field lines. *Physics of Fluids B: Plasma Physics*, 4(5):1152–1155, 1992.

[18] S. C. Guo, R. Paccagnella, and F. Romanelli. Ion-temperature-gradient-driven instability and anomalous ion heating in reversed-field pinches. *Physics of Plasmas*, 1(8):2741–2747, 1994.

Viscosity estimates in RFP fusion plasmas

[19] Chang-Chun Chen, P. H. Diamond, and S. M. Tobias. Ion heat and parallel momentum transport by stochastic magnetic fields and turbulence. *Plasma Physics and Controlled Fusion*, 64(1):015006, Dec 2021.

[20] D. Bonfiglio, L. Chacón, and S. Cappello. Nonlinear three-dimensional verification of the SPECYL and PIXIE3D magnetohydrodynamics codes for fusion plasmas. *Physics of Plasmas*, 17(8):082501, 2010.

[21] L. Chacón. An optimal, parallel, fully implicit Newton–Krylov solver for three-dimensional viscoresistive magnetohydrodynamics. *Physics of Plasmas*, 15(5):056103, 2008.

[22] M. Veranda, D. Bonfiglio, S. Cappello, G. di Giannatale, and D. F. Escande. Helically self-organized pinches: dynamical regimes and magnetic chaos healing. *Nuclear Fusion*, 60(1):016007, Oct 2019.

[23] A. M. Futch, D. Craig, R. Hesse, and C. M. Jacobson. Role of resistivity and viscosity in the excitation of stable m=0 modes during the RFP sawtooth crash. *Physics of Plasmas*, 25(11):112506, 2018.

[24] R. Fitzpatrick. Bifurcated states of a rotating tokamak plasma in the presence of a static error-field. *Physics of Plasmas*, 5(9):3325–3341, 1998.

[25] S. Chapman and T. G. Cowling. *The Mathematical Theory of Non-uniform Gases*. Cambridge University Press, 3rd edition, 1970.

[26] R. Balescu. *Transport Processes in Plasmas. Classical Transport Theory*, volume 1. North Holland, 1988.

[27] H. Goedbloed, R. Keppens, and S. Poedts. *Magnetohydrodynamics of Laboratory and Astrophysical Plasmas*. Cambridge University Press, 2019.

[28] J. J. Ramos. General expression of the gyroviscous force. *Physics of Plasmas*, 12(11):112301, 2005.

[29] A. B. Rechester and M. N. Rosenbluth. Electron heat transport in a tokamak with destroyed magnetic surfaces. *Phys. Rev. Lett.*, 40:38–41, Jan 1978.

[30] G. Spizzo, G. Pucella, O. Tudisco, M. Zuin, M. Agostini, E. Alessi, F. Auriemma, W. Bin, P. Buratti, L. Carraro, R. Cavazzana, G. Ciaccio, G. De Masi, B. Esposito, C. Galperti, S. Garavaglia, G. Granucci, M. Marinucci, L. Marrelli, E. Martines, C. Mazzotta, D. Minelli, A. Moro, M. E. Puiatti, P. Scarin, C. Sozzi, M. Spolaore, O. Schmitz, N. Vianello, and R.B. White. Density limit studies in the tokamak and the reversed-field pinch. *Nuclear Fusion*, 55(4):043007, 2015.

[31] M. Veranda, G. Spizzo, N. Vivenzi, M. Agostini, D. Bonfiglio, M. E. Puiatti, P. Scarin, D. Terranova, M. Zuin, and S. Cappello. The Greenwald density limit as a convective cell and radiative phenomenon in Reversed Field Pinch. In *Proc. of the 5$^{\text{th}}$ Asia-Pacific Conference on Plasma Physics*, remote e-conference, September 26 – October 1 2021. Division of Plasma Physics, Association of Asia-Pacific Physical Societies.

[32] P. Piovesan, D. Bonfiglio, F. Auriemma, F. Bonomo, L. Carraro, R. Cavazzana, G. De Masi, A. Fassina, P. Franz, M. Gobbin, L. Marrelli, P. Martin, E. Martines, B. Momo, L. Piron, M. Valisa, M. Veranda, N. Vianello, B. Zaniol, M. Agostini, M. Baruzzo, T. Bolzonella, A. Canton, S. Cappello, L. Chacón, G. Ciaccio, D. F. Escande, P. Innocente, R. Lorenzini, R. Paccagnella, M. E. Puiatti, P. Scarin, A. Soppelsa, G. Spizzo, M. Spolaore, D. Terranova, P. Zanca, L. Zanotto, and M. Zuin. RFX-mod: A multi-configuration fusion facility for three-dimensional physics studies. *Physics of Plasmas*, 20(5):056112, 2013.

[33] A. Alfier and R. Pasqualotto. New Thomson scattering diagnostic on RFX-mod. *Review of Scientific Instruments*, 78(1):013505, 2007.

[34] P. Innocente, S. Martini, A. Canton, and L. Tasinato. Upgrade of the RFX CO_2 interferometer using in-vessel optics for extended edge resolution. *Review of Scientific Instruments*, 68(1):694–697, 1997.

[35] L. Carraro, P. Innocente, M. E. Puiatti, F. Sattin, P. Scarin, and M. Valisa. Effects of the impurities on the loop voltage in RFX. In B. E. Keen, P. E. Stott, and J. Winter, editors, *Proc.*

*of the 22*nd *EPS Conference on Plasma Physics*, volume 19C, pages 161–164, Bournemouth, UK, 3 - 7 July 1995. European Physical Society (Petit Lancy).

[36] P. Zanca and D. Terranova. Reconstruction of the magnetic perturbation in a toroidal reversed field pinch. *Plasma Physics and Controlled Fusion*, 46(7):1115–1141, Jun 2004.

[37] L. Spitzer. *Physics of Fully Ionized Gases*. Interscience Publ., New York, 1956.

[38] M. Veranda, S. Cappello, D. Bonfiglio, D. F. Escande, and A. Kryzhanovskyy. Magnetic reconnection in three-dimensional quasi-helical pinches. *Rendiconti Lincei. Scienze Fisiche e Naturali*, 31:963–984, 2020.

[39] G. Spizzo, R. B. White, S. Cappello, and L. Marrelli. Nonlocal transport in the reversed field pinch. *Plasma Physics and Controlled Fusion*, 51(12):124026, Nov 2009.

[40] F. Auriemma, R. Lorenzini, M. Agostini, L. Carraro, G. De Masi, A. Fassina, M. Gobbin, E. Martines, P. Innocente, P. Scarin, W. Schneider, and M. Zuin. Characterization of particle confinement properties in RFX-mod at a high plasma current. *Nuclear Fusion*, 55(4):043010, Mar 2015.

[41] F. Trintchouk, M. Yamada, H. Ji, R. M. Kulsrud, and T. A. Carter. Measurement of the transverse Spitzer resistivity during collisional magnetic reconnection. *Physics of Plasmas*, 10(1):319–322, 2003.

[42] A. Kuritsyn, M. Yamada, S. Gerhardt, H. Ji, R. Kulsrud, and Y. Ren. Measurements of the parallel and transverse Spitzer resistivities during collisional magnetic reconnection. *Physics of Plasmas*, 13(5):055703, 2006.

[43] E. A. Saad and P. R. Brunsell. Experimental characterization and modelling of the resistive wall mode response in a reversed field pinch. *Plasma Physics and Controlled Fusion*, 64(5):055011, Apr 2022.

[44] G. Ciaccio, M. Veranda, D. Bonfiglio, S. Cappello, G. Spizzo, L. Chacón, and R. B. White. Numerical verification of orbit and nemato codes for magnetic topology diagnosis. *Physics of Plasmas*, 20(6):062505, 2013.